European Congress on Computational Methods
in Applied Sciences and Engineering (ECCOMAS 2012)
J. Eberhardsteiner et.al. (eds.)
Vienna, Austria, September 10-14, 2012

ENTROPY CONSERVATIVE AND ENTROPY STABLE FINITE VOLUME SCHEMES FOR MULTI-DIMENSIONAL CONSERVATION LAWS ON UNSTRUCTURED MESHES

A. Madrane[1], U. S. Fjordholm[2], S. Mishra [2] and E. Tadmor[3]

[1]Bombardier Aerospace
address
e-mail: aziz.madrane@aero.bombardier.com

[2] Seminar for Applied Mathematics, ETH Zürich
address
e-mail: {ulrikf,smishra}@sam.math.ethz.ch

[3] Department of Mathematics, University of Maryland
address
e-mail: tadmor@cscamm.umd.edu

Keywords: entropy stable,unstructured meshes,multi-dimensional,symmetrization

Abstract. *We present entropy stable schemes for the two-dimensional Euler equations on unstructured grids. We develop a novel energy conservative scheme that is very simple to implement, is computationally cheap and efficient. To allow for a correct dissipation of entropy in the vicinity of shocks, a novel numerical diffusion operator of the Roe type is designed. The entropy conservative scheme, together with this diffusion operator, gives an entropy stable scheme for Euler equations on unstructured grids. Numerical experiments are presented to demonstrate the robustness of the proposed schemes. Numerical experiments include the Sod shock tube problem, vortex advection and flow past a NACA0012 airfoil.*

1 INTRODUCTION

We deal with systems of conservation laws in several space dimensions. For simplicity of exposition, we consider the two-dimensional case in this paper. The generic form of systems of conservation laws in two space dimensions is

$$\mathbf{U}_t + \mathbf{f}_1(\mathbf{U})_x + \mathbf{f}_2(\mathbf{U})_y = 0 \tag{1}$$

with $\mathbf{U} : \Omega \times \mathbf{R}_+ \to \mathbf{R}^m$ for some $\Omega \subset \mathbf{R}^2$. Defining $\mathbf{f}(\mathbf{U}) = (\mathbf{f}_1(\mathbf{U}),\ \mathbf{f}_2(\mathbf{U}))$, we say that 1 is *hyperbolic* if the matrix $\frac{d}{d\mathbf{U}}(\mathbf{f}(\mathbf{U}) \cdot \mathbf{n})$ has m real eigenvalues for all nonzero $\mathbf{n} \in \mathbf{R}^2$. A prototypical example for 1 are the Euler equations of gas dynamics:

$$\mathbf{U} = \begin{pmatrix} \rho \\ \rho u \\ \rho v \\ \rho E \end{pmatrix}, \qquad \mathbf{f}_1(\mathbf{U}) = \begin{pmatrix} \rho u \\ \rho u^2 + p \\ \rho uv \\ (\rho E + p)u \end{pmatrix}, \qquad \mathbf{f}_2(\mathbf{U}) = \begin{pmatrix} \rho v \\ \rho uv \\ \rho v^2 + p \\ (\rho E + p)v \end{pmatrix}. \tag{2}$$

Let ρ, u, v, p, E, c and M denote the density, velocity components, pressure, internal energy, speed of sound and Mach number. For a perfect gas, the pressure, the speed of sound and the Mach number are given by

$$p = (\gamma - 1)(\rho E - \frac{1}{2}\rho(u^2 + v^2)), \quad c = \sqrt{\frac{\gamma p}{\rho}}, \quad M = \frac{\sqrt{u^2 + v^2}}{c}. \tag{3}$$

We denote $\mathbf{u} = (u,\ v)$.

1.1 Entropy framework

The solutions of 1 may develop discontinuities in finite time when even the initial data is smooth. Hence, solutions of 1 are sought in the sense of distributions. Additional admissibility criteria need to be imposed to single out unique solutions. Such criteria, called *entropy conditions*, rely on the existence of a convex function η and functions q_1, q_2 such that the following compatibility conditions hold:

$$q_1'(\mathbf{U})^\top = \eta'(\mathbf{U})^\top \mathbf{f}_1'(\mathbf{U}), \qquad q_2'(\mathbf{U})^\top = \eta'(\mathbf{U})^\top \mathbf{f}_2'(\mathbf{U}). \tag{4}$$

It is straightforward to check using 4 that *smooth* solutions of 1 satisfy an additional conservation law, the entropy identity

$$\eta(\mathbf{U})_t + q_1(\mathbf{U})_x + q_2(\mathbf{U})_y = 0. \tag{5}$$

However, entropy needs to be dissipated at shocks. Hence, the entropy identity 5 is replaced by an entropy inequality,

$$\eta(\mathbf{U})_t + q_1(\mathbf{U})_x + q_2(\mathbf{U})_y \leq 0, \tag{6}$$

that holds in the sense of distributions. The vector $\mathbf{V} = \eta'(\mathbf{U})$ is termed as the vector of *entropy variables*. The entropy inequality 6 is integrated in space to yield the stability estimate

$$\frac{d}{dt}\int_{\mathbf{R}^2} \eta(\mathbf{U}(x, y, t))dxdy \leq 0. \tag{7}$$

Given the strict convexity of the entropy function, the entropy framework through 7 provides an a priori L^2 stability estimate for the mult-dimensional system 1.

We illustrate the entropy framework for the Euler equations 2. Define the standard logarithmic entropy $s := \log(p) - \gamma \log(\rho)$. Then the entropy function and entropy fluxes for the Euler equations are given by

$$\eta(\mathbf{U}) = -\frac{\rho s}{\gamma - 1}, \quad q_1(\mathbf{U}) = -\frac{\rho u s}{\gamma - 1}, \quad q_2(\mathbf{U}) = -\frac{\rho v s}{\gamma - 1}. \tag{8}$$

The entropy variables are

$$\mathbf{V} = \left(\frac{\gamma - s}{\gamma - 1} - \frac{\rho |\mathbf{u}|^2}{p}, \ \frac{\rho u}{p}, \ \frac{\rho v}{p}, \ -\frac{\rho}{p} \right)^\top. \tag{9}$$

1.1.1 Symmetrization:

The results of Godunov and Mock show that a hyperbolic system 1 is symmetrizable if and only if it has an entropy framework. A particularly revealing form of this symmetrization is due to Barth [1]. The key to this symmetrized form is a theorem of [1] showing that for every nonzero $\mathbf{n} \in \mathbf{R}^2$, there exist suitably scaled matrix of eigenvectors $R_\mathbf{n}$ of the matrix $\frac{d}{d\mathbf{U}}(\mathbf{f}(\mathbf{U}) \cdot \mathbf{n})$ such that

$$R_\mathbf{n} R_\mathbf{n}^\top = \mathbf{U}_\mathbf{V}, \tag{10}$$

with $\mathbf{U}_\mathbf{V} = \mathbf{U}'(\mathbf{V})$ being the change-of-variables matrix from the conserved variables $\mathbf{U}$ to the entropy variables $\mathbf{V}$. This identity is independent of the direction $\mathbf{n}$, thus providing a natural scaling for the eigenvectors. Denote $R_k = R_{\mathbf{e}_k}$, with $\mathbf{e}_k$ being the unit vector in direction k, and let Λ_k be the corresponding diagonal matrix of eigenvalues. Using 10, we formally obtain

$$\begin{aligned}
\mathbf{U}_t + \mathbf{f}_1(\mathbf{U})_x + \mathbf{f}_2(\mathbf{U})_y &= \mathbf{U}_t + \mathbf{f}_1'(\mathbf{U})\mathbf{U}_x + \mathbf{f}_2'(\mathbf{U})\mathbf{U}_y, \\
&= \mathbf{U}_\mathbf{V}\mathbf{V}_t + R_1\Lambda_1 R_1^{-1}\mathbf{U}_\mathbf{V}\mathbf{V}_x + R_2\Lambda_2 R_2^{-1}\mathbf{U}_\mathbf{V}\mathbf{V}_y, \\
&= \mathbf{U}_\mathbf{V}\mathbf{V}_t + R_1\Lambda_1 R_1^\top \mathbf{V}_x + R_2\Lambda_2 R_2^\top \mathbf{V}_y.
\end{aligned}$$

As η is a convex function, $\mathbf{U}_\mathbf{V}$ is a symmetric positive definite matrix. Clearly the coefficient matrices $R_k \Lambda_k R_k^\top$ for $k = 1, 2$ are symmetric, implying that the conservation law 1 has the symmetrized form

$$\mathbf{U}_\mathbf{V}\mathbf{V}_t + R_1\Lambda_1 R_1^\top \mathbf{V}_x + R_2\Lambda_2 R_2^\top \mathbf{V}_y = 0. \tag{11}$$

For the Euler equations with the aforementioned entropy function, the change of variables matrix is given by

$$\mathbf{U}_\mathbf{V} = \begin{pmatrix} \rho & \rho\mathbf{u}^\top & E \\ \rho\mathbf{u} & \rho\mathbf{u}\mathbf{u}^\top + p\mathbf{I} & \rho H \mathbf{u} \\ E & \rho H \mathbf{u}^\top & \rho H^2 - \frac{c^2 p}{\gamma - 1} \end{pmatrix}$$

where the specific enthalpy is $H = \frac{c^2}{\gamma - 1} + \frac{|\mathbf{u}|^2}{2}$. The resulting scaled eigenvectors are

$$\begin{aligned}
r_\mathbf{n}^1 &= \sqrt{\frac{\rho(\gamma - 1)}{\gamma}} \left(n_1, \ u n_1, \ v n_1, \ \frac{(u^2 + v^2) n_1}{2} \right)^\top, \\
r_\mathbf{n}^2 &= \sqrt{\frac{\rho(\gamma - 1)}{\gamma}} \left(0, \ -\frac{c n_2}{\sqrt{\gamma - 1}}, \ \frac{c n_1}{\sqrt{\gamma - 1}}, \ -\frac{(v n_1 - u n_2) c}{\sqrt{\gamma - 1}} \right)^\top,
\end{aligned}$$

$$r^3_{\mathbf{n}} = \sqrt{\frac{\rho}{2\gamma}}\,(1,\ u+cn_1,\ v+cn_2,\ H+c(un_1+vn_2))^\top,$$
$$r^4_{\mathbf{n}} = \sqrt{\frac{\rho}{2\gamma}}\,(1,\ u-cn_1,\ v-cn_2,\ H-c(un_1+vn_2))^\top. \tag{12}$$

The diagonal matrix of eigenvalues is given by

$$\Lambda_{\mathbf{n}} = \mathrm{diag}(un_1+vn_2,\ un_1+vn_2,\ un_1+vn_2+c,\ un_1+vn_2-c). \tag{13}$$

1.2 Aims and scope of the paper.

Numerical methods to discretize systems of conservation laws, such as the Euler equations, have extensively developed in the last few decades. Of particular interest, are the finite volume methods [5] and [6], where the computational domains is divided into control volumes and a discrete (integral) version of the conservation law is imposed on each control volume. The resulting numerical fluxes are then computed by using exact or approximate solutions of the Riemann problem (in the normal direction) at each control volume interface.

It is highly desirable that a numerical scheme respects the entropy balance of the underlying PDEs. In particular, entropy should be conserved if the solutions to the conservation law are smooth and should be dissipated at shocks. However, standard numerical schemes, based on the finite volume framework, may not respect this balance. To address this, Tadmor [8] devised a framework for constructing finite difference approximations for systems of conservation laws in one space dimensions. This framework is based on two ingredients: i) an entropy conservative flux function and ii) numerical diffusion operators which dissipate entropy at shocks. The existence of entropy conservative fluxes was also shown in [8] and a set of explicit solutions were obtained in [9]. More recent papers such as [7] for the Euler equations and [2] for the shallow water equations. These explicit fluxes increase the computational efficiency of entropy conservative schemes. Arbitrarily high-order entropy stable finite difference schemes are designed in [3].

The main aim of the current paper is to extend the framework of Tadmor [8] to discretize systems of conservation laws in several space dimensions, on unstructured grids. To this end, we extend the notion of entropy conservative schemes to unstructured grids in two space dimensions as well as introduce suitable numerical diffusion operators. Explicit formulas for the Euler equations are provided. Numerical experiments (again for the Euler equations) are presented to illustrate the robustness and efficiency of the proposed schemes.

2 Discretization

2.1 Mesh description

We assume that Ω is a bounded polyhedral domain of $\mathbf{R}^2$. We introduce a conforming triangulation $\mathcal{T}_h$ in $\mathbf{R}^2$, where h is the maximal length of the edges in $\mathcal{T}_h$. For the primary grid (see Figure 1), the nodes are the vertices a_i, indexed over $i \in \mathcal{V}$, of the triangles $K \in \mathcal{T}_h$. The finite volume cells are the barycentric cells C_i, obtained by joining the midpoints M_{ij} of the sides originating at node a_i to the centroids G_{ij} of the triangles of $\mathcal{T}_h$ which meet at a_i (see Figure 2).

In the sequel we use the following notation.

Notation 2.1 *Let a_i, a_j, a_k be the three nodes defining a triangle $K \in \mathcal{T}_h$. Then*

- a_i *is the* i^{th} *vertex*
- M_{ij} *is the midpoint of side* $a_i a_j$
- $\mathcal{N}_i$ *is the set of vertices that are neighbors of node* a_i
- $|\mathcal{N}_i|$ *is the number of neighboring vertices to* a_i
- G_{ij} $(j = 1, \ldots, |\mathcal{N}_i|)$ *is the centroid of a triangle of which* a_i *is a vertex*
- C_i *is the barycentric cell constructed around* a_i
- $e_{ij} = \partial C_i \cap \partial C_j$ *is the common face of neighboring cells* C_i *and* C_j
- $\mathbf{n}_i = (n_{i_x}, n_{i_y})$ *is the outward normal vector to* ∂C_i *(see Figure 4)*
- $\mathbf{n}_{ij}^1, \mathbf{n}_{ij}^2$ *are the normals of the two components of* e_{ij} *(see Figure 3)*
- $\mathbf{U}_i^n \cong \mathbf{U}(a_i, t^n)$ *is the nodal cell average values at time* $t = t^n$.

The union of all the barycentric cells constitutes a partition of the computational domain Ω_h:

$$\Omega_h = \bigcup_{i=1}^{nv} C_i$$

where nv is the number of vertices of the original finite element triangulation $\mathcal{T}_h$. For complete details of the domain of computation for the NACA0012 airfoil in the 2D see Figure 5.

Let

$$\mathbf{n}_{ij} = \int_{\partial C_i \cap \partial C_j} \mathbf{n}\, d\sigma = \mathbf{n}_{ij}^1 + \mathbf{n}_{ij}^2$$

be the unit normal on the face $e_{ij} = G_{ij}G_{i,j+1}$ pointing out of the control volume C_i. The normal vectors $\mathbf{n}_{ij}^1$ and $\mathbf{n}_{ij}^2$ are depicted in Figure 3 and $\mathbf{n}_{ij}$ in Figure 4. Note that we have

$$\sum_{j \in \mathcal{N}_i} \mathbf{n}_{ij} = 0. \tag{14}$$

We denote the average and difference of $\mathbf{U}$ across the edge e_{ij} as

$$\overline{\mathbf{U}}_{ij} := \frac{1}{2}\left(\mathbf{U}_i + \mathbf{U}_j\right), \qquad [\![\mathbf{U}]\!]_{ij} := \mathbf{U}_j - \mathbf{U}_i,$$

and remark that $\overline{\mathbf{U}}_{ij} = \overline{\mathbf{U}}_{ji}$ and $[\![\mathbf{U}]\!]_{ij} = -[\![\mathbf{U}]\!]_{ji}$.

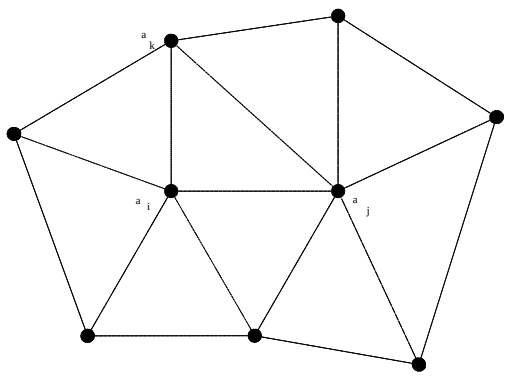

Figure 1: Primary grid

2.2 Semi-discrete finite volume scheme:

The space discretization method considered here is a vertex centered finite volume formulation. A conservative and consistant finite volume approximation of 1 is written

$$\frac{\partial \mathbf{U}_h}{\partial t} + \frac{1}{|C_i|} \sum_{j \in K(i)} \mathbf{F}(\mathbf{U}_i, \mathbf{U}_j, \mathbf{n}_{ij}) = 0. \tag{15}$$

The numerical flux $\mathbf{F}_{ij} = \mathbf{F}\left(\mathbf{U}_i, \mathbf{U}_j, \mathbf{n}_{ij}\right)$ is assumed to have the following properties:

(i) **Consistency:**

$$\mathbf{F}(\mathbf{U}, \mathbf{U}, \mathbf{n}) = \mathbf{f}(\mathbf{U}) \cdot \mathbf{n}$$

(ii) **Conservation:**

$$\mathbf{F}_{ij} = -\mathbf{F}_{ji}$$

for all $j \in \mathcal{N}_i$.

3 Entropy conservative schemes

We aim to design a numerical flux such that the resulting numerical scheme 15 is *entropy conservative* i.e, it satisfies a discrete version of the entropy identity 5. The concept of entropy conservative schemes for systems of conservation laws was introduced by Tadmor in [8] for Cartesian meshes. In this section we extend the notion of entropy conservative schemes to unstructured meshes.

Definition 3.1 *A numerical flux $\widetilde{\mathbf{F}}_{ij} = \mathbf{F}(\mathbf{U}_i, \mathbf{U}_j, \mathbf{n}_{ij})$ is* entropy conservative *if it is of the form $\widetilde{\mathbf{F}}_{ij} = \widetilde{\mathbf{F}}^1_{ij} n^1_{ij} + \widetilde{\mathbf{F}}^2_{ij} n^2_{ij}$ and the components satisfy the relations*

$$[\![\mathbf{V}]\!]^\top_{ij} \widetilde{\mathbf{F}}^k_{ij} = [\![\psi^k]\!]_{ij} \qquad k = 1, 2, \tag{16}$$

where $\psi_k(\mathbf{U}) = \mathbf{V}(\mathbf{U})^\top \mathbf{f}_k(\mathbf{U}) - q_k(\mathbf{U})$ denotes the entropy potential.

Theorem 3.2 *Let $\widetilde{\mathbf{F}}$ be an entropy conservative flux. Then the approximate solutions $\mathbf{U}_i$ computed by the finite volume scheme 15 with numerical flux $\widetilde{\mathbf{F}}$ satisfies the discrete entropy identity*

$$\frac{d}{dt}\eta(\mathbf{U}_i) + \frac{1}{|C_i|} \sum_{j \in \mathcal{N}_i} \widetilde{Q}_{ij} = 0 \tag{17}$$

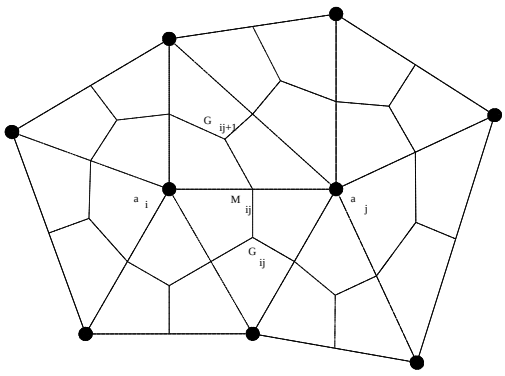

Figure 2: Barycentric cells around nodes $\mathbf{a_i}, \mathbf{a_j}$

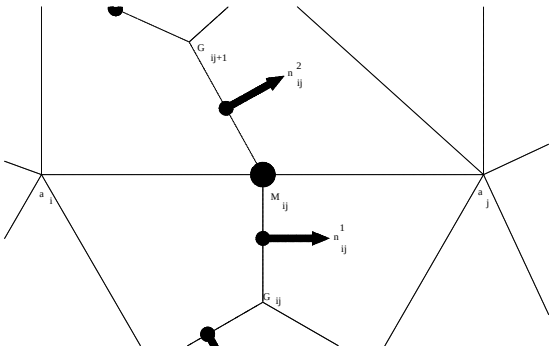

Figure 3: Part of a boundary of C_i, $e_{ij} = \partial C_i \cap \partial C_j$ and the normal vectors $\mathbf{n}_{ij}^1$ and $\mathbf{n}_{ij}^2$

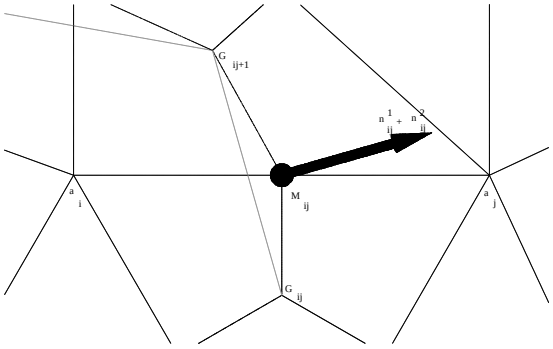

Figure 4: Part of a boundary of C_i, $e_{ij} = \partial C_i \cap \partial C_j$ and the normal vector $\mathbf{n}_{ij}$

with numerical entropy flux

$$\widetilde{Q}_{ij} := \sum_{k=1}^{2} n_{ij}^k \left(\overline{\mathbf{V}}_{ij}^\top \widetilde{\mathbf{F}}_{ij}^k - \overline{\psi^k}_{ij} \right). \tag{18}$$

Proof. Multiplying 15 by the entropy variables $\mathbf{V}_i$, we get

$$\begin{aligned}
\frac{d}{dt}\eta(\mathbf{U}_i) &= -\sum_{j\in\mathcal{N}_i} \frac{1}{|C_i|} \sum_{k=1}^{2} n_{ij}^k \mathbf{V}_i^\top \widetilde{\mathbf{F}}_{ij}^k \\
&= -\sum_{j\in\mathcal{N}_i} \frac{1}{|C_i|} \sum_{k=1}^{2} n_{ij}^k \left(\overline{\mathbf{V}}_{ij}^\top \widetilde{\mathbf{F}}_{ij}^k - \frac{1}{2} [\![\mathbf{V}]\!]_{ij}^\top \widetilde{\mathbf{F}}_{ij}^k \right) \\
&= -\sum_{j\in\mathcal{N}_i} \frac{1}{|C_i|} \sum_{k=1}^{2} n_{ij}^k \left(\overline{\mathbf{V}}_{ij}^\top \widetilde{\mathbf{F}}_{ij}^k - \frac{1}{2} [\![\psi^k]\!]_{ij} \right) \\
&= -\sum_{j\in\mathcal{N}_i} \frac{1}{|C_i|} \sum_{k=1}^{2} n_{ij}^k \left(\overline{\mathbf{V}}_{ij}^\top \widetilde{\mathbf{F}}_{ij}^k - \overline{\psi^k}_{ij} \right),
\end{aligned}$$

where we have used the identity 14 and added $\sum_{j\in\mathcal{N}_i} \sum_{k=1}^{2} \frac{1}{|C_i|} n_{ij}^k \psi_i^k = 0$.

We note that the condition 16 provides a single algebraic equation for m unknowns. In general, it is not clear whether a solution of 16 exists. Furthermore, the solutions of 16 will not be unique except for scalar equations. In [8], Tadmor showed the existence of at least one solution of 16 for any system of conservation laws. Explicit solutions were constructed in [9]. However, the entropy conservative fluxes of [9] are computationally expensive; see [2]. Instead,

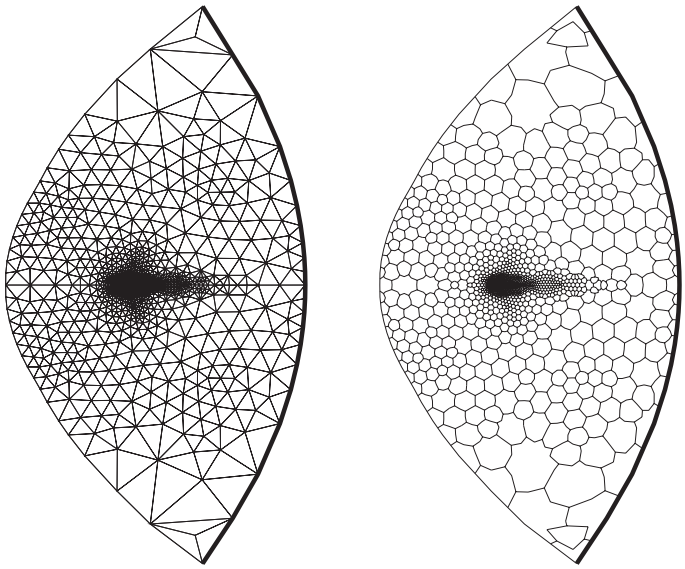

Figure 5: NACA0012 airfoil, Primary grid and barycentric cell C_i

we follow recent papers [2, 7] to obtain algebraically simple and computational inexpensive solution of 16. For concreteness we consider the Euler equations of gas dynamics 2.

Denote by Z the so-called Roe parameter vector

$$Z = \sqrt{\frac{\rho}{p}} = \begin{pmatrix} 1 \\ u \\ v \\ p \end{pmatrix}.$$

It is readily verified that

$$\rho = Z_1 Z_4, \quad p = \frac{Z_4}{Z_1}, \quad u = \frac{Z_2}{Z_1}, \quad v = \frac{Z_3}{Z_1}, \quad m_1 = \rho u = Z_2 Z_4, \quad m_2 = \rho v = Z_3 Z_4$$

Denoting by $s = \log(p) - \gamma \log(\rho)$ the standard logarithmic entropy, we have

$$s = \ln\left(\frac{Z_4^{(1-\gamma)}}{Z_1^{(1+\gamma)}}\right), \qquad \eta(\mathbf{U}) = \frac{-Z_1 Z_4 s}{\gamma - 1}.$$

The entropy variables are

$$\mathbf{V} = \begin{pmatrix} \frac{\gamma - S}{\gamma - 1} - \frac{m_1^2 + m_2^2}{2p\rho} \\ \frac{m_1}{p} \\ \frac{m_2}{p} \\ -\frac{\rho}{p} \end{pmatrix} = \begin{pmatrix} \frac{\gamma}{\gamma-1} + \ln(Z_4) + (\frac{1+\gamma}{1-\gamma}) \ln Z_1 - \frac{Z_2^2 + Z_3^2}{2} \\ Z_1 Z_2 \\ Z_1 Z_3 \\ -Z_1^2 \end{pmatrix},$$

the entropy fluxes are

$$q_1(\mathbf{U}) = \frac{-m_1 S}{\gamma - 1} = \frac{-Z_2 Z_4 S}{\gamma - 1}, \qquad q_2(\mathbf{U}) = \frac{-m_2 S}{\gamma - 1} = \frac{-Z_3 Z_4 S}{\gamma - 1}$$

and the entropy potentials are

$$\psi_1(\mathbf{U}) = m_1, \qquad \psi_2(\mathbf{U}) = m_2.$$

Upon solving 16 we get the entropy conservative fluxes

$$\widetilde{\mathbf{F}}_1 = \begin{pmatrix} \widetilde{\mathbf{F}}_1^1 \\ \widetilde{\mathbf{F}}_1^2 \\ \widetilde{\mathbf{F}}_1^3 \\ \widetilde{\mathbf{F}}_1^4 \end{pmatrix} = \begin{pmatrix} \bar{Z}_2 Z_4^{\ln} \\ \frac{\bar{Z}_4 + \widetilde{F}^{1,1}\bar{Z}_2}{\bar{Z}_1} \\ \frac{\bar{Z}_2 \bar{Z}_3 Z_2^{\ln}}{\bar{Z}_1} \\ \frac{\frac{\gamma+1}{\gamma-1}\frac{1}{Z_1^{\ln}}\widetilde{F}_1^1 + \bar{Z}_2\widetilde{F}_1^2 + \bar{Z}_3\widetilde{F}_1^3}{2\bar{Z}_1} \end{pmatrix}$$

and

$$\widetilde{\mathbf{F}}_2 = \begin{pmatrix} \widetilde{\mathbf{F}}_2^1 \\ \widetilde{\mathbf{F}}_2^2 \\ \widetilde{\mathbf{F}}_2^3 \\ \widetilde{\mathbf{F}}_2^4 \end{pmatrix} = \begin{pmatrix} \bar{Z}_3 Z_4^{\ln} \\ \frac{\bar{Z}_2 \widetilde{F}_2^1}{\bar{Z}_1} \\ \frac{\bar{Z}_4 + \widetilde{F}_2^1 \bar{Z}_3}{\bar{Z}_1} \\ \frac{\frac{\gamma+1}{\gamma-1}\frac{1}{Z_1^{\ln}}\widetilde{F}_2^1 + \bar{Z}_2\widetilde{F}_2^2 + \bar{Z}_3\widetilde{F}_2^3}{2\bar{Z}_1} \end{pmatrix}.$$

Here, $a^{\ln}$ is the logarithmic mean defined as

$$a^{\ln} = \frac{[\![a]\!]}{[\![\log(a)]\!]}$$

See [7] for further details.

4 Entropy stable schemes for Euler equations

4.1 Numerical diffusion operators

The entropy conservative schemes lead to unphysical oscillations near shocks. We need to add numerical diffusion to eliminate these oscillations. Following the procedure of [2], we consider numerical flux functions

$$\mathbf{F}_{ij} = \widetilde{\mathbf{F}}_{ij} - \frac{1}{2}\mathbf{D}_{ij}[\![\mathbf{V}]\!]_{ij}. \tag{19}$$

Here, $\widetilde{\mathbf{F}}$ is an entropy conservative flux and $\mathbf{D}$ is any symmetric positive definite matrix with $\mathbf{D}_{ij} = \mathbf{D}_{ji}$. The flux $\mathbf{F}_{ij}$ is consistent because $\mathbf{U}_i = \mathbf{U}_j$ implies that $\mathbf{F}_{ij} = \widetilde{\mathbf{F}}_{ij} - 0 = \mathbf{f}(\mathbf{U}_i)\cdot\mathbf{n}_{ij}$, and it is conservative because $\mathbf{F}_{ji} = \widetilde{\mathbf{F}}_{ji} - \frac{1}{2}\mathbf{D}_{ji}\left(-[\![\mathbf{V}]\!]_{ij}\right) = -\left(\widetilde{\mathbf{F}}_{ij} - \frac{1}{2}\mathbf{D}_{ij}[\![\mathbf{V}]\!]_{ij}\right) = -\mathbf{F}_{ij}$.

The scheme with numerical flux 19 is entropy stable by the following lemma.

Lemma 4.1 *Let the numerical flux in the finite volume scheme 15 be defined by 19. Then the approximate solutions $\mathbf{U}_i$ computed by the scheme 15 satisfy the discrete entropy inequality*

$$\frac{d}{dt}\eta(\mathbf{U}_i) + \sum_{j\in N_i}\frac{1}{|C_i|}Q_{ij} \le 0, \tag{20}$$

with numerical entropy flux Q given by

$$Q_{ij} = \widetilde{Q}_{ij} - \frac{1}{2}\overline{\mathbf{V}}_{ij}^{\top}\mathbf{D}_{ij}[\![\mathbf{V}]\!]_{ij},$$

where $\widetilde{Q}$ is defined in 18. Summing over $i \in \mathcal{V}$, we obtain the entropy bound

$$\frac{d}{dt}\sum_{i\in\mathcal{V}}\eta(\mathbf{U}_i) \leq 0. \tag{21}$$

Poof Multiplying the finite volume formulation 15 by $\mathbf{V}_i$ we get

$$\begin{aligned}
\frac{d}{dt}\eta(\mathbf{U}_i) &= -\sum_{j\in\mathcal{N}_i}\frac{1}{|C_i|}\left(\mathbf{V}_i^\top\widetilde{\mathbf{F}}_{ij} - \frac{1}{2}\mathbf{V}_i^\top\mathbf{D}_{ij}[\![\mathbf{V}]\!]_{ij}\right)\\
&= -\sum_{j\in\mathcal{N}_i}\frac{1}{|C_i|}\left(\widetilde{Q}_{ij} - \frac{1}{2}\left(\overline{\mathbf{V}}_{ij}^\top - \frac{1}{2}[\![\mathbf{V}]\!]_{ij}^\top\right)\mathbf{D}_{ij}[\![\mathbf{V}]\!]_{ij}\right)\\
&= -\sum_{j\in\mathcal{N}_i}\frac{1}{|C_i|}Q_{ij} - \frac{1}{4}\sum_{j\in\mathcal{N}_i}\frac{1}{|C_i|}[\![\mathbf{V}]\!]_{ij}^\top\mathbf{D}_{ij}[\![\mathbf{V}]\!]_{ij}\\
&\leq -\sum_{j\in\mathcal{N}_i}\frac{1}{|C_i|}Q_{ij},
\end{aligned}$$

thus proving 20.

4.2 Specifying the numerical diffusion matrix.

Following [2, 3], we choose the following numerical diffusion matrix:

$$\mathbf{D}_{ij} = R_{\mathbf{n}_{ij}}|\Lambda_{\mathbf{n}_{ij}}|R_{\mathbf{n}_{ij}}^\top. \tag{22}$$

Here, $\Lambda_{\mathbf{n}}$ and $R_{\mathbf{n}}$ are the matrix of eigenvalues and eigenvectors as defined in 10. The matrices can be evaluated at the average state $\overline{\mathbf{U}}_{ij}$.

5 Numerical experiments

5.1 Vortex advection

We start testing the scheme on a smooth test case for the two-dimensional Euler equations. This test case involves long time simulation. The initial data is set in terms of velocity u and v, the temperature $\theta = \frac{p}{\rho}$ and entropy $s = \log p - \gamma\log\rho$:

$$u = 1 - (y - y_c)\phi(r), \quad v = 1 - (x - x_c)\phi(r), \quad \theta = 1 - \frac{\gamma - 1}{2\gamma}\phi(r)^2$$

where $r = \sqrt{(x - x_c)^2 + (y - y_c)^2}$ with (x_c, y_c) being the initial center of the vortex, and

$$\phi(r) = \epsilon e^{\alpha(1-\tau^2)}, \quad \tau = \frac{r}{r_c}$$

We set the free parameters, $\epsilon = \frac{5}{2\pi}$, $\alpha = \frac{1}{2}$, $r_c = 1$ and $(x_c, y_c) = (5, 5)$. The exact solution of this initial value problem is simply $\mathbf{U}(x, y, t) = \mathbf{U}(x - t, y - t, 0)$. In other words, the initial vortex centered at (x_c, y_c) is advected diagonally with a velocity of 1 in the x- and y-directions. The computational domain and initial data is shown in Figure 6. We compute up to $T = 30$ on a mesh with 40836 vertices. Figures 7,8 show the computed density at the time $t = 30$ using the entropy conservative scheme and the standard Roe scheme. Figure 9 shows that there is a significant gain in accuracy using the entropy conservative scheme as compared to the Roe scheme.

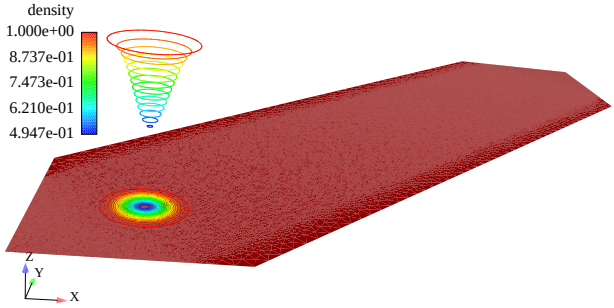

Figure 6: Computational domain with initial data, with slices in z-direction

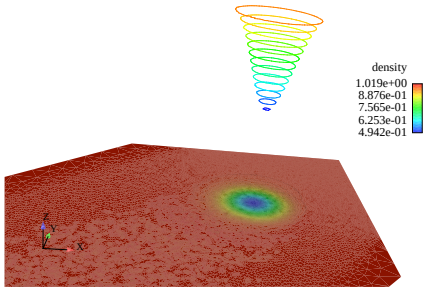

Figure 7: Entropy conservative scheme, ρ at $t = 30$ with slices in z-direction.

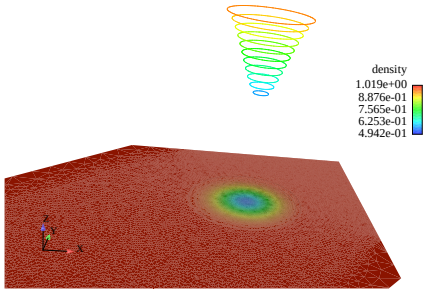

Figure 8: Roe schemeρ at $t = 30$ with slices in z-direction.

5.2 Sod shock tube in two dimensions

We consider the Euler Equations in the computational domain $\Omega = [0, 1] \times [0, 0.1]$ with Riemann initial data

$$\begin{aligned} (\rho, m_1, m_2, l)_{left} &= (1, 0, 0, 2.5) \qquad 0 < x < 0.5 \\ (\rho, m_1, m_2, l)_{right} &= (0.125, 0, 0, 0.25) \qquad 0.5 < x < 1. \end{aligned}$$

The initial discontinuity breaks into a left-going rarefaction wave, a right-going shock and a right-going contact discontinuity. The computed solution with the entropy conservative scheme at time $T = 1.4$ on a mesh of 20136 points, shown in Figures 10 and 11. The computed solution

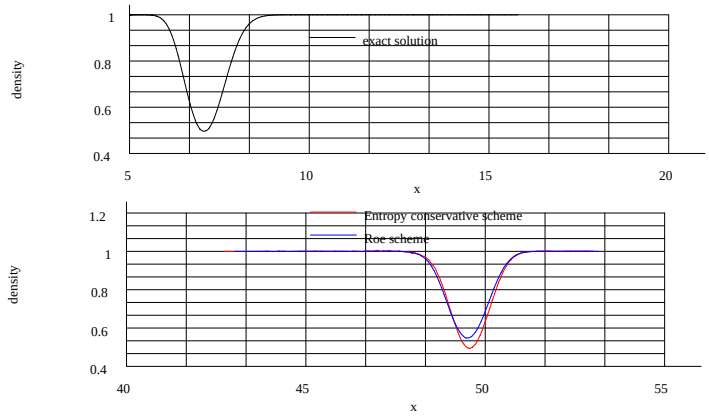

Figure 9: A one-dimensional cut for the vortex advection problem/ Entropy conservative scheme vs Roe scheme, ρ at $t = 30$. Exact solution in red line.

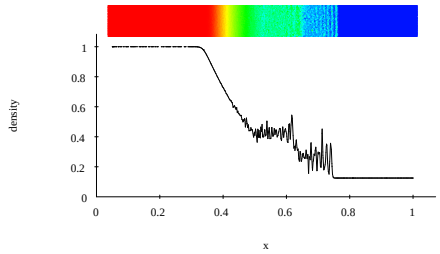

Figure 10: Density for the 2-D Sod shock tube problem. Entropy conservative scheme.

with this scheme has significant oscillations. This is to expected as the scheme preserves the entropy (see figure 13), whereas the entropy of the exact solution has to be dissipated at the shock wave. The failure to dissipative this entropy results in oscillations at the mesh scale. To remove these oscillations, we use the entropy stable scheme developed in the previous section. Now, the entropy is dissipated as shown in figure 14. Furthermore, the scheme resolves the shock wave, the contact discontinuity and the rarefaction wave without any spurious oscillations, see Figure 12. A comparison with the standard Roe scheme is also shown in figure 12. The total entropy $\sum_{i\in\mathcal{V}} |C_i|\eta(\mathbf{U})_i$ versus time is shown in Figures 13 and 14.

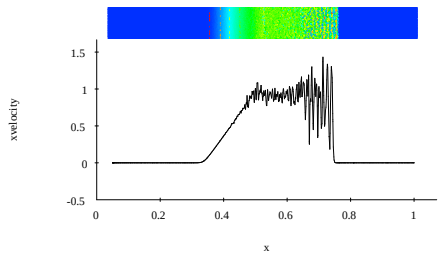

Figure 11: Velocity for the 2-D Sod shock tube problem. Entropy conservative scheme.

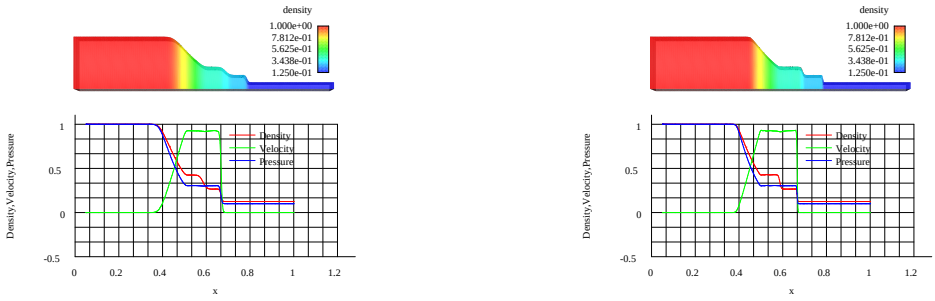

Figure 12: Solutions for the 2-D Sod shock tube problem computed with the entropy stable scheme and the Roe scheme.

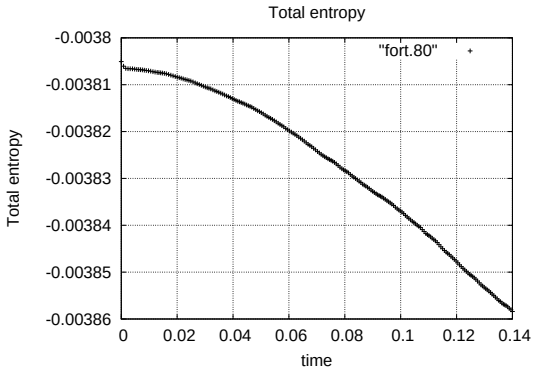

Figure 13: Total entropy vs. time, (Entropy conservative scheme)

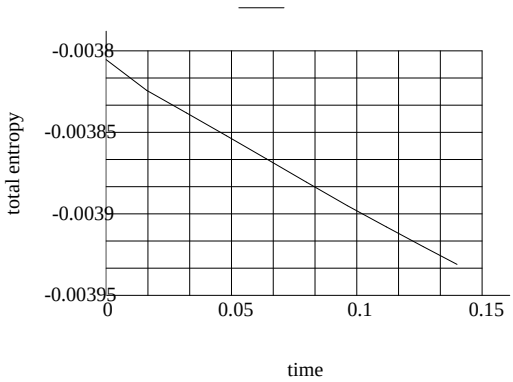

Figure 14: Total entropy vs. time, (Entropy stable conservative scheme)

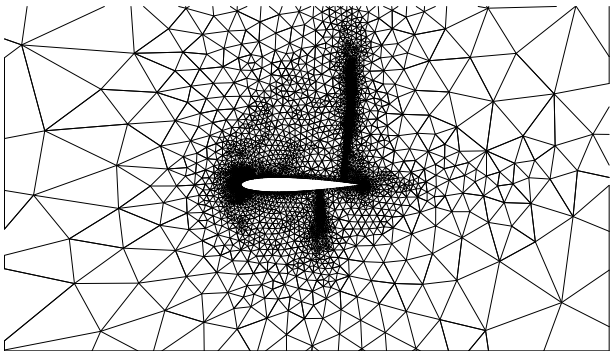

Figure 15: Adapted mesh

5.3 Simulation of transonic flows around a NACA 0012 airofoil

We consider a transonic flow around a NACA0012 at angle of attack $\alpha = 1^o$ and Mach number at infinity $M_\infty = 0.85$. We have selected this problem since it is a quite classical and significant test problem for Euler solvers [4]. Figure 15 shows the final adapted triangulation near the profile used to solve the test problem. The mesh contains 14930 points. Figures 16, 17 show the pressure and density lines for the entropy stable scheme and Roe scheme. We can observe the similar shocks locations obtained with the two schemes implying a small difference in pressure distributions shown in Figure 18.

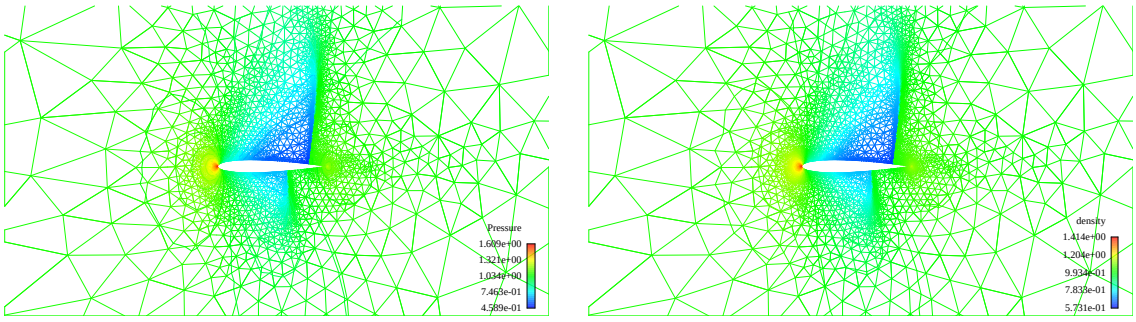

Figure 16: Iso-pressure and density lines,(entropy stable scheme)

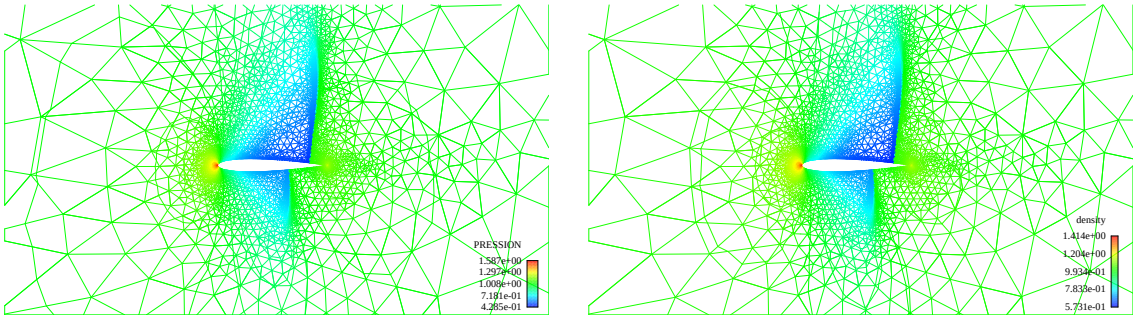

Figure 17: Iso-pressure and density lines, (Roe scheme)

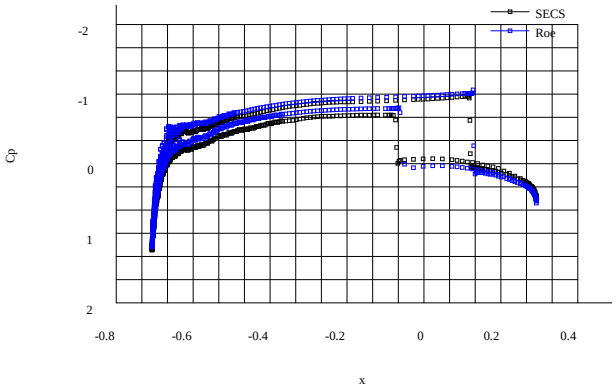

Figure 18: Pressure distribution (entropy stable scheme vs. Roe scheme)

6 Conclusion

We have presented in this paper a new formulation of entropy conservative and entropy stable schemes on unstructured grids for the stable numerical solution of Euler equations modelling transonic, supersonic and hypersonic flows. With these methods we can simulate 3-D flows around complex geometries such as complete aircraft.

REFERENCES

[1] T.J. BARTH, *Numerical methods for gaz-dynamics systems on unstructured meshes. In An introduction to Recent Developments in Theory and Numerics of Conservation Laws pp 195-285. Lecture Notes in Computational Science and Engineering Volume 5, Springer, Berlin. Eds D. Kroner, M. Ohlberger and Rohde, C., 1999*

[2] U.S. FJORDHOLM, S. MISHRA AND E. TADMOR, *Energy preserving and energy stable schemes for the shallow water equations. "Foundations of Computational Mathematics", Proc. FoCM held in Hong Kong 2008 (F. Cuckers, A. Pinkus and M. Todd, eds), London Math. Soc. Lecture Notes Ser. 363, pp. 93-139, 2009.*

[3] U.S. FJORDHOLM, S. MISHRA AND E. TADMOR, *Arbitrary high-order accurate entropy stable essentially non-oscillatory schemes for systems of conservation laws. SIAM Jl. Num. Anal, to appear.*

[4] GAMM WORKSHOP ON NUMERICAL SIMULATION OF COMPRESSIBLE EULER FLOWS, *France, 10-13 June 1986.*

[5] C. HIRSCH, *Numerical Computation of Internal and External Flows, Vol-2: Computational Methods for Inviscid and Viscous Flows, Wiley Series in Numerical Methods in Engineering, J. Wiley & Sons, 1990.*

[6] P. ARMINJON, M.C. VIALLON AND A. MADRANE, *A Finite Volume Extension of the Lax-Friedrichs and Nessyahu-Tadmor Schemes for Conservation Laws on Unstructured Grids*, revised version with numerical applications, Int. J. of Comp. Fluid Dynamics (1997), Vol. 9, No. 1, 1-22.

[7] F. ISMAIL AND P. L. ROE, *Affordable, entropy-consistent Euler flux functions II: Entropy production at shocks. J. Comput. Phys., vol. 228, issue 15 (2009), pp. 5410–5436.*

[8] E. TADMOR, *The numerical viscosity of entropy stable schemes for systems of conservation laws*, I. Math. Comp., 49, 91-103, 1987.

[9] E. TADMOR, *Entropy stability theory for difference approximations of nonlinear conservation laws and related time–dependant problem*, Acta Numerica (2003), pp. 451–512.